Numerical investigation of tip leakage vortex cavitation

IOP Conf. Series: Earth and Environmental Science **240** (2019) 072003 doi:10.1088/1755-1315/240/7/072003

Numerical investigation of tip leakage vortex cavitation

Ali Maghooli, Mehrdad Raisee, Seyed Ahmad Nourbakhsh

Hydraulic Machinery Research Institute, School of Mechanical Engineering, College of Engineering, University of Tehran, P.O.Box 11155-4563, Tehran, Iran

mraisee@ut.ac.ir

Abstract. Tip leakage vortex cavitation is a concern for axial hydraulic turbines. Generally, cavitation may occur in the core of the TLV, often leading to erosion of the runner blades and the casing. The objective of this paper is to study the effects of this phenomenon on the hydrodynamics characteristics of a standard NACA0009 blade. Numerical simulations of the present study are carried out using the ANSYS CFX. The k–ω SST turbulence model and the Schnerr-Sauer cavitation model are respectively used for the modeling of turbulence and cavitation. In the first step of this study, the effect of considering cavitation phenomenon and transient state is investigated by monitoring the coordinate of the vortex core center and comparing them with the experimental data. The steady state simulation with cavitation modeling leads to acceptable prediction of vortex core center position and the unsteady cavitation modeling further improved the accuracy of the predictions. The influence of tip clearance, incidence angle and cavitation number on the hydrodynamics characteristics of the hydrofoil is further studied. The results demonstrate that incidence angle and cavitation number have more pronounced effects on improving the lift to drag ratio in comparison to the tip clearance. According to performance curves, the maximum lift coefficient is obtained by incidence angle of 12 degree in the cavitation number range of $1<\sigma<1.25$.

1. Introduction

In order to ensure blade rotation without rubbing, axial turbines require a small clearance, between the tip of the blades and the casing. The tip clearance is usually kept as small as possible within the limits of manufacturing constraints. In hydraulic machines, the tip clearance is typically 0.1% of the blade chord [1]. However, the tip leakage vortex is formed in this specific region and cavitation develops in the low-pressure region that prevails in the core of TLVs as well as in the clearance region. This phenomenon causes erosion, observed in the tip of the blades. Negative consequences of tip leakage flow cavitation and its influences on performance of turbomachines has been studied extensively in the literature. Subjects include efficiency losses [2, 3], rotating instabilities [4, 5, 6] and also cavitation in pump and inducers [7, 8]. Astolfi et al. [9] proposed an empirical equation to estimate minimum pressure value in the tip region. Recognition of minimum pressure value in tip region indicates the possibility of cavitation occurrence. Roussopoulos and Monkewitz [1], investigated the position and strength of the vortex on the suction side of a Kaplan-type turbine blade with various endings, using particle image velocimetry (PIV). They found that the greatest danger of cavitation erosion exists when the casing of the turbine is of the "semi-spherical" type. Drayer [10] studied the dynamics of TLV cavitation and the gap width effects on it comprehensively, using PIV and laser doppler velocimetry (LDV) instruments. He proposed some guides to displace the cavitation away from the blade. The results of this investigation

led to some new numerical investigations including Zhao et al. [11], Decaix et al. [12, 13], Gue et al. [14] and Zhang et al. [15]. Zhao et al. [11] proposed and utilized a new cavitation model for the computations of the developed tip leakage vortex cavitating flows. Compared with the conventional model, better agreement was observed between the new model and experiment. Decaix et al. [12, 13] and Gue et al. [14] studied the influence of turbulence models on accuracy of numerical predictions. They reported that the k-ω SST model was the best turbulent model considering accuracy of the results and calculation costs. Zhang et al. [15] investigated the onset and development of TLV cavitation and its effects on characteristic curves in an axial flow pumps. Numerical results show that the TLV cavitation cloud in the axial flow pump mainly includes tip clearance cavitation, shear layer cavitation, and TLV cavitation.

The subject of this paper is to emphasize on considering cavitation phenomenon and transient state while modeling TLV flow and demonstrate its influence on performance curves of a standard blade. For this purpose, the vortex is simulated for a NACA0009 blade in a water tunnel, while the tip clearance, incidence angle and cavitation number are varied.

2. Computational details

2.1. Test case

The test case investigated in the current paper is chosen based on the experiments of Drayer [10]. The schematic of the computational domain, boundary conditions and details of dimensioning is demonstrated in figure 1. The test section is a water tunnel with a 150×150mm^2 square cross-section and 750mm length. A NACA0009 hydrofoil with a chord of 100mm, the maximum thickness of 10mm is used and a clearance length is considered as a variable parameter.

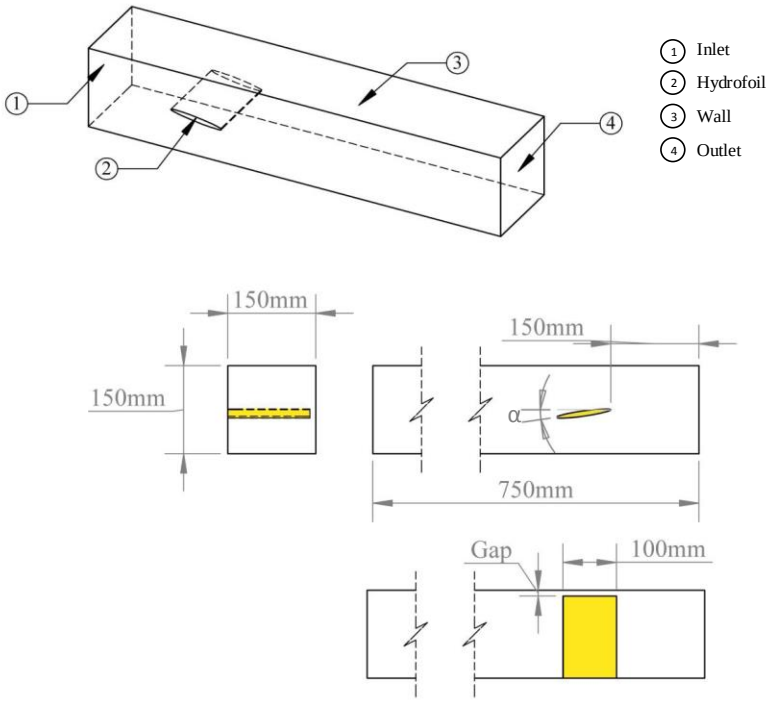

Figure 1. Top: Domain and boundary conditions. Bottom: Details of dimensioning.

The ratio of clearance between the hydrofoil tip and the water tunnel wall to the hydrofoil thickness (h) is the normalized gap width (τ) which varies between 0.2 and 2 in the experiment. In addition, four incidence angles of $\alpha = 3^o, \alpha = 5^o, \alpha = 7^o$ and $\alpha = 10^o$ are chosen in the experiment. The third

variable parameter is cavitation number $\sigma = \frac{P_\infty - P_v}{\frac{1}{2}\rho U_\infty^2}$, which vary between 0.25 and 3. It should be noted that, in this work cavitation number is adjusted by varying the outlet pressure P_∞.

2.2. Numerical method and boundary conditions

In this work, the numerical predictions are obtained using ANSYS CFX. The Reynolds-averaged Navier-Stokes (RANS) in conjunction with the $k-\omega$ SST turbulence model are employed for the computations. In addition, the Schnerr-Sauer model was applied as cavitation model and the high resolution scheme is used for the approximation on nonlinear convection terms in all transport equations. Convergence is specified as RMS residuals of 10^{-5}.

According to the experimental conditions, a uniform velocity $W_\infty = 10\, m/s$ is set as inlet and the static pressure is adjusted as outlet. The hydrofoil and water tunnel are considered as solid wall with no slip condition.

2.3. Computational Grid

The computational grid consists of hexahedral cells is generated using ANSYS ICEM with a relatively high mesh resolution near the TLV region, leading edge and trailing edge of the blade. With reference to Zhao et al. [11], a computational grid with 70 nodes in the gap region is employed for the numerical simulations. Moreover, in this paper several grid dependency studies have been performed to ensure that the numerical predictions in this paper do no depend to the mesh size. In the following a sample of such studies is provided. Considering the condition of $\tau = 1$, $\alpha = 10^\circ$ and $\sigma = 1$, the predicted y-coordinate of the vortex center using different meshes in a z-plane (i.e. $z/c = 1$ downstream of the hydrofoil shown in figure 2. is displayed in figure 3. As can be observed, a fine computational mesh with 2.5×10^6 cells is fine enough to yield-independent results. The numerical results presented in the subsequent sections of this paper are obtained with this mesh size. Figure 4. indicates the computational mesh for two important regions of the field.

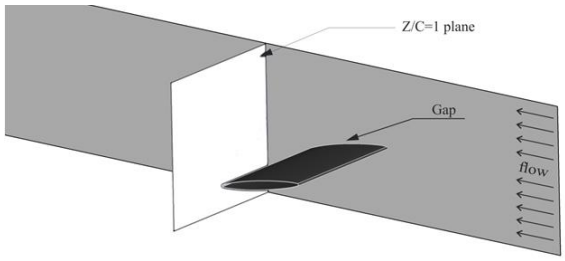

Figure 2. Position of plane $z/c = 1$ in the computational domain.

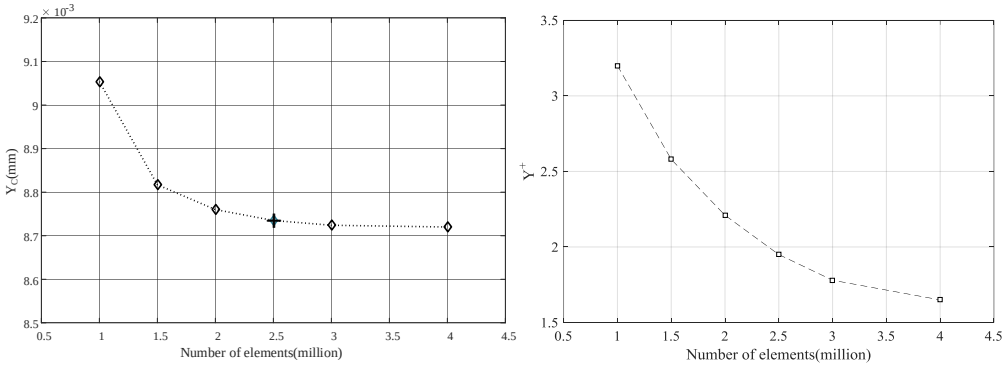

Figure 3. Grid sensitivity study for the: left: vortex center vertical position at plane $z/c = 1$. Right: Grid Y^+ at tip region.

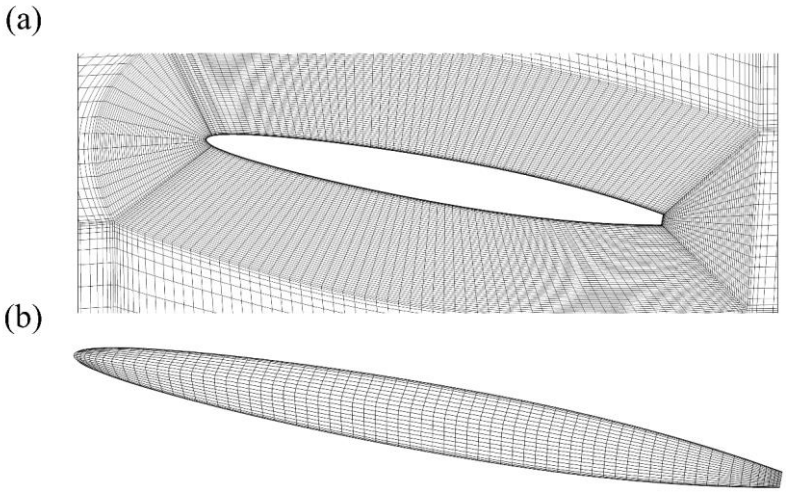

Figure 4. a) Boundary layer mesh around hydrofoil. b) Tip mesh.

3. Results and discussion

In the following, first the numerical predictions are compared with the reported experimental. Then, the effects of clearance size, incidence angle and cavitation number are presented and discussed.

3.1. Comparison of numerical results with the experimental data

In the current paper, the numerical simulations are performed in three steps. In the first step, only a steady state and non-cavitating simulation is conducted. In the second stage, the steady state computation by considering the cavitation is carried out. Finally, in the third step, unsteady calculations by taking into account the cavitation phenomenon are accomplished. The objective is to understand how considering these physical features can improve the numerical predictions. For this propose, the influence of considering cavitation phenomenon is first investigated by comparing the results of steps 1 and 2. Then, the numerical results of steps 2 and 3 are compared.

It is expected that neglecting the cavitation in a flow yields less accurate results. To assess this natural expectation, in figure 5. the steady-state predictions of y-coordinate of the vortex center for cavitating and non-cavitating flows are compared with the measurements. Computations were carried out for two angle of incidences of $\alpha = 7^{\circ}$ (left figure) and 10° (right figure) and normalized gap widths of $\tau = 0.2, 0.3, 0.4, 0.5, 0.7, 1, 1.5$ and 2. Consistent with the experiment conditions, the ambient pressure and fluid velocity are respectively set at $P_{\infty} = 1\ atm$ and $W_{\infty} = 10\ m/s$ in the simulations. The measurements show that by increasing the gap width the center of vortex shifts downward but a reverse trend occurs by increasing the angle of incidence. It is noted that both sets of computations reproduced the trend of experimental data. However, as can be observed, computations of non-cavitation flow largely overestimates the vertical coordinate of the vortex center. On the other hand, considering cavitation phenomenon in the computations leads to significant improvements in the numerical predictions at both angles of incidence especially at $\alpha = 7^{\circ}$. As a physical point of view, it is clear that the improvement of numerical predictions is a result of considering the cavitation cloud at vortex core which affect the vortex structure significantly. The existence of vapor at vortex center could alter the physical properties of the fluid, which in turn leads to more accurate numerical results.

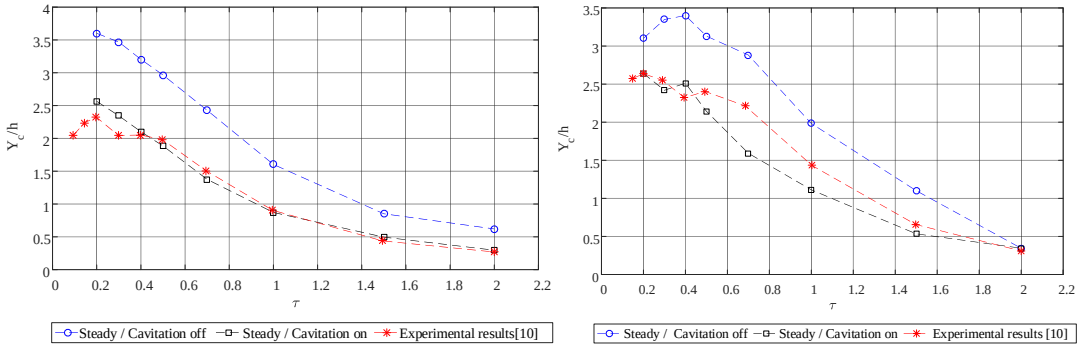

Figure 5. Comparison of numerical results of vortex vertical center position for steps 1 and 2 with experimental results (Drayer [10]). Left: $\alpha = 7^{\circ}$. Right: $\alpha = 10^{\circ}$.

Having discussed the steady state predictions, attention is now focused on unsteady computations. In figure 6, unsteady predictions for vertical position (Y_C) of vortex center in plane $z/c = 1$ are compared with the experimental data of Drayer [10]. The steady state predictions are also included for comparison. As can be seen for the smaller angle of incidence, differences between steady and unsteady results are minor and both steady and unsteady results are in excellent accord with the experimental data. For the larger angle of incidence, the difference between steady and unsteady results are higher and the unsteady results are in closer agreement with the measured data. It is worth mentioning that Gue et al. [14] has shown that considering the flow unsteadiness in TLV cavitation modeling does not significantly improve the numerical predictions.

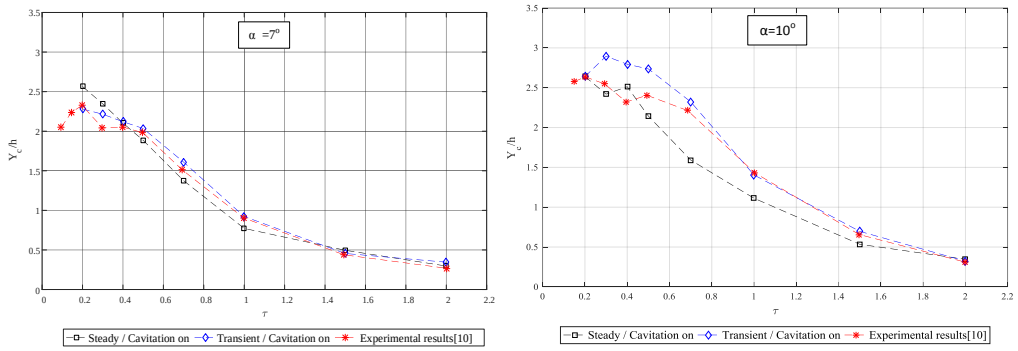

Figure 6. Comparison of numerical results of vortex vertical center position for steps 2 and 3 with experimental results (Drayer [10]). Left: $\alpha = 7^{\circ}$. Right: $\alpha = 10^{\circ}$.

In figure 7. the measured and computed vorticity contours and streamlines for three incidence angles of $5^{\circ}, 7^{\circ}$ and 10° are compared. Comparisons are presented in a square region of 40×40 mm^2 surrounding the TLV generated by the hydrofoil in planes $z/c = 1, 1.2$ and 1.5. As can be observed, the angle of incidence has a pronounced impact on the TLV characteristics and structure. While the vortex structures for incidence angles of 5° and 7° are more or less similar, the incidence angle of 10° appears to generate a more complex vortex structure. For the 10° incidence angle vortex deforms helically as the particles roll up into the vortex. It is noted that the numerical predictions of TLV characteristics are qualitatively similar to those measured. The intensity of vorticity at the center of the TLV is somewhat underpredicted by the computations.

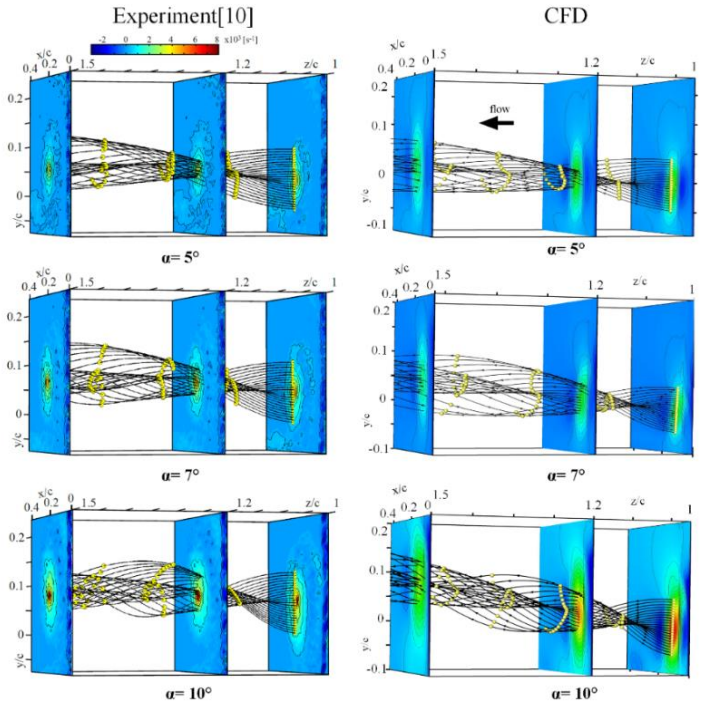

Figure 7. Comparison of CFD simulations and experimental results (Drayer [10]) for 3D Streamlines and contours of the streamwise vorticity, for three z-planes z/c=1, 1.2, 1.5.

3.2. Effects of clearance size, incidence angle and Cavitation number

Tip leakage vortex cavitation formation and development depends on several parameters such as tip clearance size, the incidence angle and the Cavitation number which will be further investigated in this subsection. As described by Drayer [10], the clearance size plays a key role in TLV cavitation unset and development. More specifically, a wider clearance causes a greater flow leakage and thus drops of the performance. On the other hand, tight clearance may result in direct contact of rotor blades and casing a well as friction problems in the tip of the blade. To examine, the effects of gap clearance on the hydrodynamics performance, simulations were carried out for conditions given in Table 1.

Table 1. Conditions considered for investigating the effect of tip clearance.

Operating pressure	0.7 atm
Incidence angle(α)	$3^{\circ}, 5^{\circ}, 7^{\circ}, 10^{\circ}$
Tip clearance(τ)	$0.2, 0.3, 0.4, 0.5, 0.7, 1, 1.5, 2$

The variation of lift coefficient ($C_L = F_L / \frac{1}{2}\rho A W_\infty^2$) versus clearance size for different incidence angles is plotted in figure 8. In general, at first the lift coefficient is slightly decreases with the gap size. However, for large clearances (i.e. $\tau > 0.7$) the lift coefficient does not change with the clearance size at all angles of incidence. As expected, the lift coefficient is increased with increase in incidence angle.

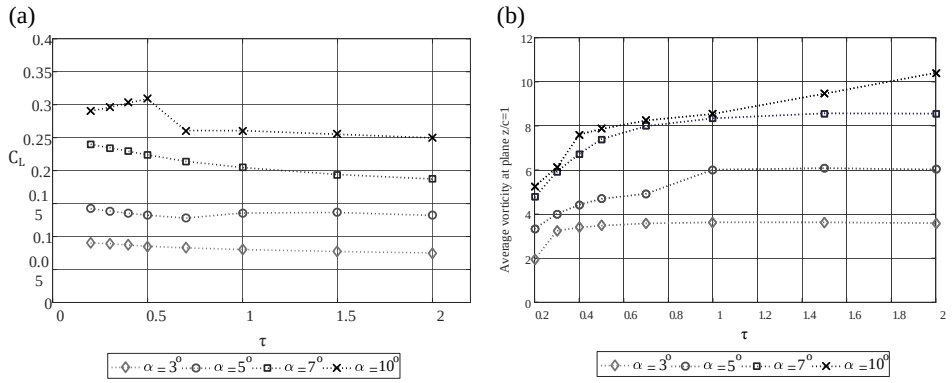

Figure 8. a) Lift coefficient. b) Average vorticity at plane z/c=1, in terms of clearance size for different incidence angles.

In addition to the lift coefficient, the clearance size will affect the flow field kinematic quantities. figure 8.b. shows the average vorticity at plane z/c=1 against the clearance width. It is clear that increasing the tip clearance causes a stronger swirling flow downstream of the hydrofoil. It is noted that for $\tau \geq 1$ increasing in gap does not affect the average vorticity in all incidence angles except $\alpha = 10^{\circ}$.

As already shown in figure 7, another important parameter which has a pronounced impact on the TLV characteristics is incidence angle. To study the effects of incidence on the aerodynamic performance of the blade, simulations with different conditions (given in Table 2) were carried out. Two important hydrodynamics performance quantities namely; the lift coefficient and the drag coefficient ($C_D = F_D / \frac{1}{2}\rho A W_{\infty}^2$) are calculated for each case. Figure 10. and figure 11. show the distribution of these quantities versus incidence angle for different operating pressures.

Table 2. Conditions considered for investigating the effect of incidence angle.

Operating pressure	0.5, 1, 1.5 atm
Incidence angle(α)	$3^{\circ}, 4^{\circ}, 5^{\circ}, 6^{\circ}, 7^{\circ}, 8^{\circ}, 9^{\circ}, 10^{\circ}, 11^{\circ}, 12^{\circ}, 13^{\circ}, 14^{\circ}, 15^{\circ}$
Tip clearance(τ)	1.5

Figure 9.a. shows the lift coefficient against incidence angle of the blade. It is clear that all three curves have a peak value at incidence angle of $\alpha = 12^{\circ}$ and variation in operating pressure does not affect it. Moreover, for a fixed incidence angle, the maximum lift coefficient is obtained for the operating pressure of $P_{\infty} = 1$ atm as will be shown in figure 11. profoundly.

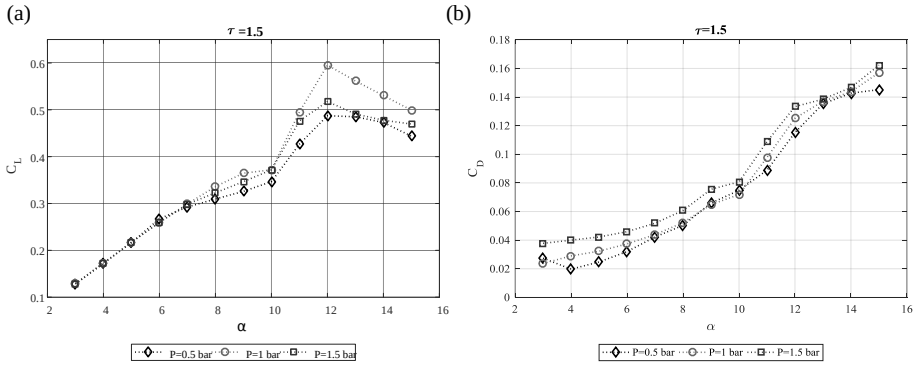

Figure 9. a) Lift coefficient b) Drag coefficient, versus incidence angle for three operating pressures.

Figure 9.b. illustrates the calculated drag coefficient against the incidence angle of the blade. According to this graph, for all three operating pressures, the rise in incidence angle results in an increase in the drag coefficient. It is noted that the maximum drag coefficient occurs at the operating pressure of $P_\infty = 1.5$ atm for each incidence angle.

Cavitation number is the most important parameter in cavitating flows which determines the possibility of occurrence of cavitation. On the other hand, cavitation occurrence will affect the aerodynamic performance of the blade. The influence of cavitation number on the performance of the blade is investigated by varying the Cavitation number between 0.25 and 3 as indicated in Table 3.

Table 3. Conditions considered for investigating the effect of Cavitation number.

Inlet velocity (W_∞)	10 m/s
Cavitation number (σ)	0.25, 0.5, 0.75, 1, 1.25, 1.5, 2, 3
Incidence angle (α)	10°
Tip clearance (τ)	1

Figure 10. shows how cavitation number will affect the lift coefficient of the blade. According to this figure, the maximum lift coefficient will be obtained for $\sigma = 1$ and for lower Cavitation numbers, the lift coefficient is quickly dropped. For $\sigma > 1.25$ the lift coefficient is slowly decreased.

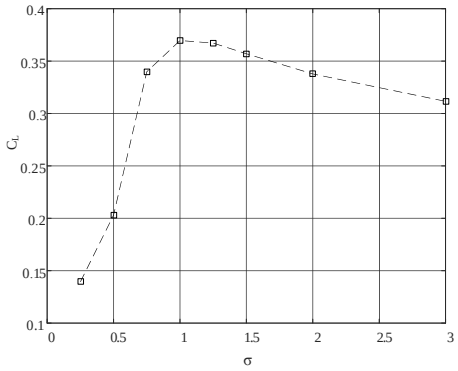

Figure 10. Lift coefficient versus cavitation number.

In order to reach a deeper understanding about the effect of cavitation number it is necessary to examine pressure distribution around the hydrofoil which is demonstrated in figure 11.a. at tip of the hydrofoil. As it shown, cavitation number plays a key role on pressure distribution. Therefore, it can be concluded that the lift coefficient is affected consequently. According to this figure for $\sigma = 0.5$ and 0.75 the pressure distributions at leading edge are different. In fact cavitation onset at leading edge causes a significant pressure drop in this region. This feature is more pronounced at the middle of the hydrofoil (figure 11.b.). Of course in this region the pressure distribution is affected by another cavitation mode which is known as leading edge cavitation (Drayer [10]) and is not mentioned in this paper.

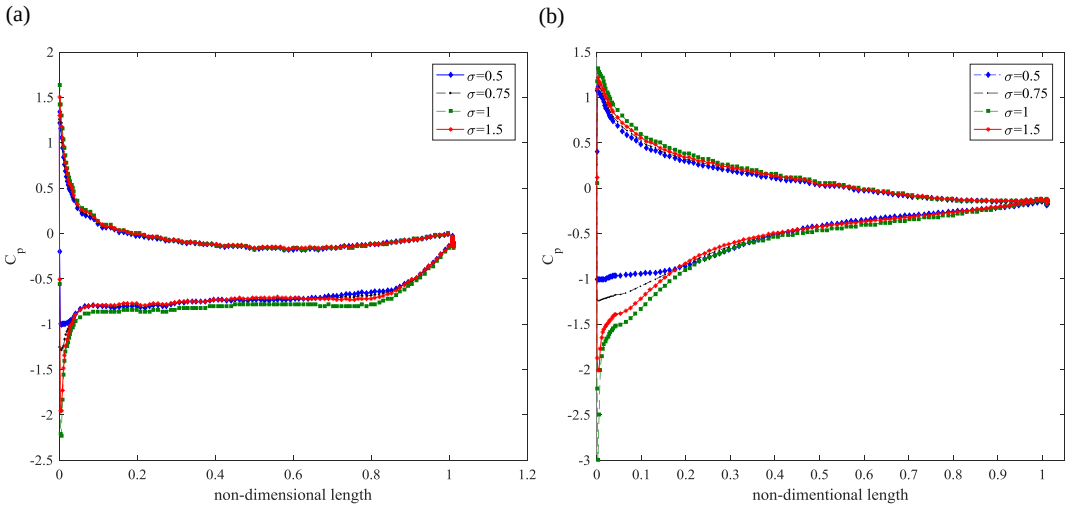

Figure 11. Pressure distribution around hydrofoil for two different section. a) at Tip. b) in the middle

Figure 12. demonstrates the effect of cavitation number on the drag coefficient of the blade. As shown, the drag coefficient is increased by an increase in Cavitation number. It is noted that for $0.75 < \sigma < 1.25$ the drag coefficient remains constant. To reach a final conclusion, it is interesting to focus on the behavior of lift to drag ratio against Cavitation number curve as shown in figure 12. From the results shown in this figure, it can concluded that $1 < \sigma < 1.25$ is the most appropriate range for Cavitation number.

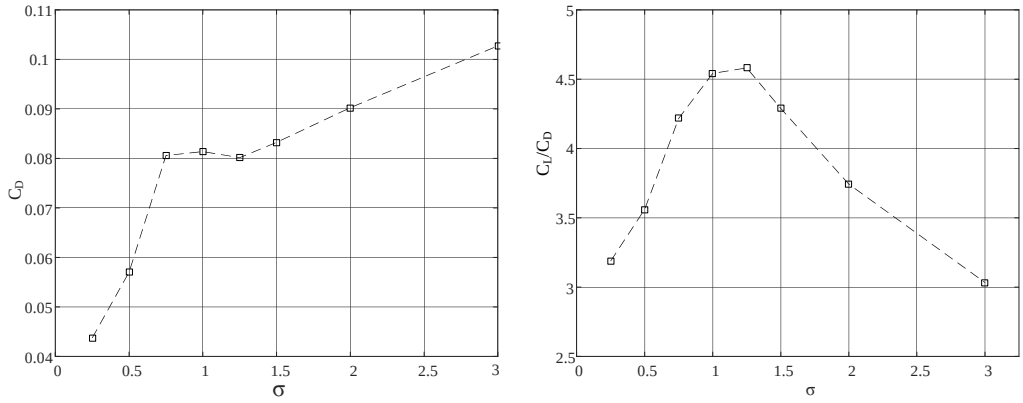

Figure 12 Blade performance for different cavitation numbers. Left: drag coefficient. Right: lift to drag coefficient.

4. Conclusion

In this study, calculations of the tip leakage vortex cavitation around the tip of a standard NACA0009 hydrofoil are performed. It is shown that for accurate prediction of investigated flow, it is necessary to carry out unsteady simulations and more importantly take into account the cavitation phenomena's in the simulations. In addition, the effects of three important parameters tip clearance size, incidence angle and cavitation number on the hydrodynamics characteristics are investigated. Based on the computations, the following conclusions can be drawn:

- The lift coefficient slightly decreases with the gap size. However, for larger clearances (i.e. $\tau >$ 0.7) the lift coefficient does not change with the clearance size. Similarly, for the same range of clearance size, this parameter does not affect the average vorticity at plane z/c=1.
- Incidence angle has the most pronounced effect on TLV cavitation formation and performance of the blade. The numerical results show that the formation of tip leakage vortex is significantly

affected by incidence angle. In addition, according to performance curves, the lift coefficient has a maximum value for incidence angle of $\alpha = 12^{\circ}$ and variation in operating pressure does not affect it. Moreover, the increase in incidence angle results in an increase the drag coefficient.

- Finally, the effect of cavitation number on performance of the blade is investigated. The simulations were carried out for a range of cavitation number $0.25 \leq \sigma \leq 3$. According to figure 11, pressure distribution around the hydrofoil is influenced by cavitation number and consequently the performance of the blade is affected. In general, it can be concluded that $1 \leq \sigma \leq 1.25$ is the most appropriate range for cavitation number.

References

[1] Roussopoulos K and Monkewitz P A 2000 Measurements of Tip Vortex Characteristics and the Effect of an Anti-Cavitation Lip on a Model Kaplan Turbine Blade 119–44
[2] Denton J Do 1993 Loss mechanisms in turbomachines *ASME 1993 International Gas Turbine and Aeroengine Congress and Exposition* (American Society of Mechanical Engineers) p V002T14A001-V002T14A001
[3] Xiao X, McCarter A A and Lakshminarayana B 2000 Tip clearance effects in a turbine rotor: part I—pressure field and loss *ASME Turbo Expo 2000: Power for Land, Sea, and Air* (American Society of Mechanical Engineers) p V001T03A047-V001T03A047
[4] Kang D, Arimoto Y, Yonezawa K, Horiguchi H, Kawata Y, Hah C and Tsujimoto Y 2010 Suppression of cavitation instabilities in an inducer by circumferential groove and explanation of higher frequency components *Int. J. Fluid Mach. Syst.* **3** 137–49
[5] Song S J and Martinez-Sanchez M 1997 Rotordynamic forces due to turbine tip leakage: Part I—blade scale effects *J. Turbomach.* **119** 695–703
[6] Song S J and Martinez-Sanchez M 1997 Rotordynamic forces due to turbine tip leakage: Part II—radius scale effects and experimental verification *J. Turbomach.* **119** 704–13
[7] Laborde R, Chantrel P and Mory M 1997 Tip clearance and tip vortex cavitation in an axial flow pump *J. Fluids Eng.* **119** 680–5
[8] Farrell K J and Billet M L 1994 A Correlation of Leakage Vortex Cavitation in Axial-Flow Pumps *J. Fluids Eng.* **116** 551–7
[9] Astolfi J-A, Fruman D H and Billard J-Y 1999 A model for tip vortex roll-up in the near field region of three-dimensional foils and the prediction of cavitation onset *Eur. J. Mech. B/Fluids* **18** 757–75
[10] Dreyer M 2015 Mind The Gap : Tip Leakage Vortex Dynamics and Cavitation in Axial Turbines PAR **6611**
[11] Zhao Y, Wang G, Jiang Y and Huang B 2016 Numerical analysis of developed tip leakage cavitating flows using a new transport-based model *Int. Commun. Heat Mass Transf.* **78** 39–47
[12] Decaix J, Balarac G, Dreyer M, Farhat M and Münch C 2015 *RANS computations of tip vortex cavitation* vol 656
[13] Decaix J, Balarac G, Dreyer M, Farhat M and Münch C 2015 RANS and LES computations of the tip-leakage vortex for different gap widths *J. Turbul.* **16** 309–41
[14] Guo Q, Zhou L and Wang Z 2016 Numerical evaluation of the clearance geometries effect on the flow field and performance of a hydrofoil *Renew. Energy* **99** 390–7
[15] Zhang D, Shi L, Shi W, Zhao R, Wang H and van Esch B P M 2015 Numerical analysis of unsteady tip leakage vortex cavitation cloud and unstable suction-side-perpendicular cavitating vortices in an axial flow pump *Int. J. Multiph. Flow* **77** 244–59